Am J Cancer Res 2020;10(7):2043-2065
www.ajcr.us /ISSN:2156-6976/ajcr0112358

Original Article

Repurposing antidepressant sertraline as a pharmacological drug to target prostate cancer stem cells: dual activation of apoptosis and autophagy signaling by deregulating redox balance

Somaiah Chinnapaka, Velavan Bakthavachalam, Gnanasekar Munirathinam

Department of Biomedical Sciences, College of Medicine, University of Illinois, Rockford, IL, USA

Received April 11, 2020; Accepted May 14, 2020; Epub July 1, 2020; Published July 15, 2020

Abstract: Cancer stem cells play a major role in tumor initiation, progression, and tumor relapse of prostate cancer (PCa). Recent studies suggest that Translationally Controlled Tumor Protein (TCTP) is a critical survival factor of stem cells including cancer stem cells. Here, we aimed to determine whether the TCTP inhibitor sertraline (STL) could target prostate cancer stem cells (PCSC). In colony formation, spheroidogenesis, angiogenesis, and wound healing assays STL showed a robust inhibition of tumorigenic (colony growth), angiogenic (endothelial tube formation) and metastatic (wound healing and migration) potential of PCSC. Interestingly, antioxidants such as N-acetyl cysteine (NAC), Glutathione (GSH) and catalase effectively blocked the cytotoxicity effect of STL on PCSC implicating oxidative stress as the underlying anti-PCSC targeting mechanism. Cell cycle analysis showed a robust G_0 arrest in PCSC exposed to STL. Notably, STL induced both apoptosis and autophagy by activating free radical generation, hydrogen peroxide formation (H_2O_2), lipid peroxidation (LPO) and depleted the levels of glutathione (GSH). Moreover, surface marker expression analysis using confocal revealed that STL significantly down regulates the expression levels of aldehyde dehydrogenase 1 (ALDH1) and cluster of differentiation 44 (CD44) stem cell markers. Furthermore, in western blot analysis, STL treatment applied in a dose-dependent manner, caused a marked decrease in TCTP, phospho TCTP, anti-apoptotic markers survivin and cellular inhibitor of apoptosis protein 1 (cIAP1) expression as well as a significant increase in cleaved caspase3 and cleaved Poly [ADP-ribose] polymerase 1 (PARP-1) expression. Of note, STL also significantly down regulated the stem cell markers (ALDH1 and CD44) and epithelial to mesenchymal transition (EMT) markers such as transcription factor 8 (TCF8) and lymphoid enhancer-binding factor-1 (LEF1) expression levels. Concurrently, STL increased the levels of autophagy markers such as light chain (LC3), Beclin1 and autophagy-related gene (ATG5). Taken together, our study suggests that STL could be an effective therapeutic agent in eliminating prostate cancer stem cells.

Keywords: Sertraline, antidepressant, TCTP, prostate cancer stem cells, prostate cancer, oxidative stress, angiogenesis, autophagy, apoptosis

Introduction

Prostate cancer (PCa) is the second leading cause of cancer related deaths among men in the United States [1]. The traditional therapies available for PCa includes prostectomy, radiation, hormonal deprivation therapy and chemotherapy [2]. Most of the therapies are not effective in treating metastatic or advanced PCa patients. In majority of cases, cancer therapies fail due to an incomplete eradication of tumor cells, resulting in tumor relapse [3].

The cancer stem cell model hypothesis explains the molecular characteristics of oncological disease state, cancer cell progression and development. These cells are responsible for tumor relapse and drug resistance [4]. Cancer stem cells have self-renewal capacity to produce same type of cancer stem cells and undergo differentiation to produce a heterogenous tumor cell population [5].

Cancer stem cells are found to be resistant to current chemotherapy and their characteristics such as slow growth, multidrug resistance, and high expression of anti-apoptotic proteins that make them resistant to the conventional therapies. Novel therapies should be developed to target both the tumor bulk and cancer stem

cells [6-9]. Cancer treatment that is more effective against cancer can be achieved by specifically targeting cancer stem cells rather than the conventional anti-proliferative strategies, which are aimed at destructing the tumor bulk.

Cancer diagnosis can have a huge impact on cancer patients, families and caregivers. Cancer patients commonly experience depression, anxiety and fear for life changing events, which is reported to be higher in cancer patients compared to normal individual. Lack of sleep in cancer patients affect the cancer treatment outcome. Stress is defined as an emotional or physical tension and it can come in any form of events such as anger, depression, frustration and nervousness [10]. Generally, stress is mediated by epinephrine, nor epinephrine catecholamine, glucocorticoids, growth factors and inflammatory molecules such as cytokines [11]. It is also known to affect immunological, endocrine, physiological and behavioral functions [12].

Epidemiological and clinical studies revealed that cancer progression is associated with stress, lack of social support and depression [13, 14]. Depression is associated with high incidence of mortality rates in cancer patients [15, 16]. *In-vitro* and *in-vivo* studies have shown that stress related process can impact the signaling pathways related to cancer evolution and immune modulation [17]. Evidence from literature suggests that depression is associated with cancer progression [18-20]. In an experimental study, mice with anxiety chronic stress was shown to be more susceptible to chemically induced tumor formation [21].

Antidepressants are group of neurotransmitter modulators that are commonly used medication for treating depression. The most commonly used antidepressants are selective serotonin reuptake inhibitor (SSRI) [22], tricyclics [23], monoamine oxidase inhibitors [24], serotonin-noradrenaline reuptake inhibitors [25]. SSRI are safer and well tolerated than other antidepressant drugs [26]. The percentage of SSRI prescriptions are reported to be high in USA. Serotonin is one of the chemical messenger, which acts as a neurotransmitter that carries signals between brain cells. SSRI drugs are specific to serotonin and they do not affect other neurotransmitters in the brain.

It has been documented that antidepressants such as clomipramine and SSRI (paroxetine and fluoxetine), act as an anti-proliferative agents in addition to their psychotropic effect [27]. Antidepressants sertraline (STL) and fluoxetine reported to induce cell death in various cancer models such as glioma [28], neuroblastoma [29], acute myeloid leukemia [30] and mouse melanoma cell lines [31]. In particular, STL has been shown to be effective against wide range of cancers such as medulloblastoma [32], lymphoma [33], melanoma [34], and acute myeloid leukemia [30].

From earlier studies, it was evidenced that antidepressant STL targets Translationally Controlled Tumor Protein (TCTP) at molecular level [35, 36] and TCTP is a well-known therapeutic target in various cancer models [34, 36-39]. TCTP expression levels regulate tumor progression and metastasis in cholangiocarcinoma [40]. It has been reported that TCTP induces Epithelial-mesenchymal transition (EMT) [41-43] and responsible for tumor progression [41-43]. Deregulation of TCTP expression was observed in various cancers including PCa [38]. Interestingly, TCTP over expression is seen in cancer stem cell compartment which in turn activates autophagy via mammalian target of rapamycin (mTOR) and deregulating p53 signaling pathways [36]. Downregulation of TCTP expression has been successfully achieved with antidepressant STL for melanoma treatment [34]. Dihydroartemisinin (DIART), antimalarial drug also suppress the expression levels of TCTP in esophageal cancer [44], breast cancer [45], and PCa [46]. Therefore, in our study we first compared the effect of TCTP-targeting drugs STL with antimalarial drug DIART and based on the potency results, we aimed to investigate the therapeutic effects of STL on PCSC. The underlying anticancer mechanism and anti-cancer effect of STL in PCSC is not known. In this study, we have evaluated the anti-PCSC targeting effects of STL on PCSC proliferation, *In vitro* tumorigenesis, and metastasis properties while also delineating its anticancer mechanism.

Materials and methods

Cell lines

The human PCSC (Celprogen) were cultured in fibronectin (FBN) coated flasks and grown in

human prostate stem cell complete growth media with serum and antibiotics (Celprogen, USA). The source of PCSC was from human prostate cancer tissue established at Celprogen [65, 66]. This cell line is positive for markers such as CD44, CD133, SSEA3/4, Oct4, Aldehyde dehydrogenase, and Telomerase. Human Fibronectin (FBN) was procured from Sigma. PC3, DU145, LNCaP and HUVEC/TERT2 cell lines were obtained from ATCC, Manassas, VA, USA. PC3, DU145 and LNCaP were cultured and maintained in RPMI1640 with 10% of fetal calf serum, 30 µg/ml antimycotic and 20 µg/ml gentamycin. HUVEC/TERT2 was cultured in vascular cell basal medium supplemented with Endothelial Cell Growth Kit-BBE (ATCC). All cell lines were maintained at 37°C and 5% CO_2.

Chemicals and inhibitors

Sertraline and deferoxamine was purchased from Acros Organics and dihydroartemisinin was obtained from AK Scientific. Antioxidants N-Acetyl cysteine, Glutathione and catalase were purchased from Sigma Chemicals. 4,4 dimethyl-3-thiosemicarbazone (Thermo Fischer Scientific), and Ferrostatin (Apex Biotechnology) were used as iron modulators.

Cell viability assay

PCSC were seeded at a density of 3×10^3 cells/well in a 96-well plate and cultured with sertraline (STL) and dihydroartemisinin (DIART) at various doses (1, 2.5, 5, 10, 25 and 50 µM) in the presence or absence of antioxidants (NAC, GSH and catalase). Chelators such as 4,4 dimethyl-3-thiosemicarbazone (DPP44MT) 100 nM, deferoxamine (DFO) 50 µM, and Ferrostatin (FS) 50 µM were combined with STL and incubated for 48 hrs. Effects of STL were also tested on the cell viability of prostate cancer cell lines PC3, DU145 and LNCaP for 48 hrs. After treatment, 3-(4,5-dimethylthiazol-2-yl)-2,5-diphenyl tetrazolium bromide (MTT) reagent obtained from Sigma was added to each well, and the cells were cultured for additional 3 hrs at 37°C and 5% CO_2. Upon incubation, the media was removed, and 100 µl solubilization solution containing Triton-X100 (Sigma) and isopropanol (1:10) from Millipore was added into each well. The absorbance was then read at 570 nm in a microplate reader (Biotech Synergy 2) [47].

Colony formation assay

500 PCSC cells/well were seeded onto FBN coated 6-well plate and incubated at 37°C. After 24 hrs, cells were treated with different concentrations of STL for 2 weeks. Following treatment, cells were fixed with acetic acid: methanol (1:7) and stained with 0.05% crystal violet (Fischer Scientific). Colonies were counted and images were captured (Olympus 1X73) as described previously [47].

Spheroid assay

PCSC were seeded on to low attachment plates (Corning) with the seeding density of 500 cells per well in a 6-well plate. After 24 hrs, cells were treated with varying concentrations of STL and incubated for 1 week. The cells were stained with Calcein green (50 µM) obtained from Fischer Scientific and images were captured using fluorescence microscope (Olympus IX73). Size of the spheroid were determined using ImageJ software.

Angiogenesis assay

Briefly, 1×10^5 HUVEC with or without STL (10, 25 and 50 µM) containing media were seeded onto 96 well plate coated with matrigel and the cells were incubated at 37°C for 6 hrs. After incubation, tube formation was documented using microscope (Olympus IX73) [47].

Wound healing assay

PCSC (10000 cells/well) were seeded onto 24-well plates coated with FBN and allowed the cells to reach 90-100% confluence. After confluence, scratch was made using 200 µl pipette tip and washed with 1×PBS. The cells were incubated with media containing various concentrations of STL (10, 25 and 50 µM) for 24 hrs. Images were captured at initial (0 hr) and end point (24 hrs) of wound healing assay. Wound healing gap was measured using T-Scratch software [47].

Transwell migration assay

PCSC cells (3×10^5) in serum free media were seeded onto transwell inserts (Millipore, Billerica, MA, USA) with or without STL and allowed them to migrate for 24 hrs. Epidermal growth factor (hEGF) (5 ng/ml) were added to the bot-

tom chamber containing complete media. Non migrated cells from upper side of the transwell insert was removed using cotton swab. The cells present in the bottom side of the insert and cells migrated to bottom well of the chamber were fixed with 4% paraformaldehyde and stained with 0.05% crystal violet. Stained cells were counted and images were captured using Olympus IX73 microscope. The stained cells were counted and the percentage of migrated cells were determined [47].

Apoptosis assay

PCSC were seeded at a density of 1×10^6 cells/well in a 6-well plate and cultured with STL (10, 25 and 50 μM) for 48 hrs. Subsequently, the cells were collected and stained with Annexin V-fluorescein isothiocyanate (FITC) and propidium iodide (PI) (BD Biosciences) according to the manufacturer's instructions. Apoptosis was analyzed using flow cytometry (FACS Calibur, BD Biosciences, Mountain View, CA) [39].

Cell cycle analysis

Briefly, 3×10^5 PCSC were seeded onto 25 cm^2 flasks and incubated at 37°C. After 24 hrs, cells were treated with different doses of STL and incubated for 48 hrs. After treatment, both live and dead cells were collected and spun down using centrifugation 1000 g for 5 min. Cells were fixed with 70% ice cold ethanol and stained with 100 μg/ml PI (Sigma) and analyzed using flow cytometry (FACS Calibur; BD Biosciences, Mountain View, CA) [47].

Reactive oxygen species (ROS) level detection

PCSC cells were seeded at a density of 1×10^6 cells/well in a 6-well plate and cultured with STL (10, 25 and 50 μM) for 48 hrs. Subsequently, the cells were incubated with 10 μM 2',7'-dichlorodihydrofluorescein diacetate (H2DCFDA) (Sigma-Aldrich) at 37°C for 30 min. ROS activation was detected using fluorescence microscope (Olympus IX73 microscope). Fluorescence intensity was quantified using ImageJ software [47].

MitoSox staining

Fluorescence microscopy analysis: 8-well chamber slides were coated with FBN (10 ng/cm^2) and incubated at 37°C for 1 hr. PCSC (1×10^5) were seeded onto FBN coated 8-well chambers and incubated at 37°C. After 24 hrs, PCSC were treated with different concentrations of STL for 6 hrs and stained with Mitosox Red (Invitrogen) at a concentration of 5 μM and incubated for 30 min at 37°C. Mitosox levels were observed using fluorescence microscope (Olympus IX73). Fluorescence intensity was quantified using ImageJ software [47].

Flow cytometry quantification: PCSC (1×10^5) were seeded onto FBN coated 6-well plate and treated with varying concentrations of STL for 4 hrs. Following incubation, cells were collected and stained with 5 μM of Mitosox red for 30 min and analysed using flow cytometry (FACS Calibur, BD Biosciences, Mountain View, CA). Data was quantified using FlowJo software [47].

Hydrogen peroxide (H_2O_2) assay

Hydrogen peroxide assay was performed according to the manufacture instructions (Bio Vision, Hydrogen peroxide assay kit). Briefly, PCSC (3×10^5) were seeded on to T-25 flasks and treated with different doses of STL (10, 25 and 50 μM) for 6 hrs and incubated at 37°C. After incubation, culture media supernatants were collected and centrifuged for 1000 g for 15 min. Following centrifugation, the supernatant was filtered using 10 kDa MW spin filter (Biovision). Next, 50 μl of sample were mixed with 50 μl of reaction mix and incubated for 10 min at room temperature. The excitation and emission of fluorescence (excitation/emission = 535/587 nm) was read in spectrophotometer (Biotech Synergy 2). Standard curve was plotted to determine the levels of H_2O_2 in test samples and reaction mixture served as a blank [47].

Thiobarbituric acid reactive species assay (TBARS)

Thiobarbituric acid reactive species assay (TBARS) was performed to check the lipid peroxidation amount in PCSC upon STL treatment according to manufacturer's instructions (Cayman Chemical TBARS Assay Kit). Briefly, PCSC (1×10^5) were seeded onto FBN coated flasks and incubated at 37°C and treated with various doses of STL (10, 25 and 50 μM) for 6 hrs. After treatment, cells were collected and centrifuged 1000 g for 5 min. Supernatant was discarded and the pellet was suspended in a 1 ml of culture medium and were subjected to sonication

on ice. Following sonication, 100 µl of lysate was mixed with 100 µl of sodium dodecyl sulphate (SDS) and 4 ml of thiobarbituric acid and heated for 1 hr at 75°C. Next, the samples were incubated on ice for 10 min and centrifuged for 10 min with 1600 g at 4°C. Fluorescence was measured at an excitation wavelength of 530 nm and an emission wavelength of 550 nm in spectrophotometer (Biotech Synergy 2). Reaction mixture was served as a blank control. A standard curve was plotted and identify the lipid peroxidation in the form of malondialdehyde (MDA) concentration (µM) [47].

Glutathione assay

Glutathione assay (Cayman Chemical glutathione assay kit) was performed to quantitate the levels of reduced glutathione (GSH) and oxidized glutathione (GSSG) [48]. The enzyme glutathione reductase was used to measure the GSH content in the glutathione assay. In enzymatic assay, reduced glutathione reacts with a colorless DTNB (5,5'-dithio-bis-2-(nitrobenzoic acid) substrate to produce a yellow colored TNB (5-thio-2-nitrobenzoic acid) product. The production of TNB is associated with formation of GSH and the absorbance was measured at 405-414 nm using spectrophotometer. For this, PCSC (1×10^5) were seeded onto FBN coated flasks and treated with various doses of STL for 6 hrs. Following treatment, live and dead cells were collected and centrifuged at 1000 g for 5 min. After centrifugation, cell pellet was suspended in 2 ml of ice cold buffer was added and sonicated. After sonication, cell lysate was centrifuged at 12000 g for 15 min at 4°C. Supernatants were collected and used for the assay.

Confocal microscopy

PCSC cells (1×10^5) were seeded onto FBN coated 8-well chambers and treated with different doses of STL (10, 25 and 50 µM). After 48 hrs of treatment, cells were fixed with 4% paraformaldehyde (Fischer scientific) for 15 min and permeabilized with 0.1% Triton-X-100 (Acros Organics) for 15 min following washes. After incubation, slides were washed with 1X phosphate buffer saline (PBS) and blocking with 5% BSA for 1 hr. Next, the cells were incubated with primary antibody such as ALDH1 and CD44 which were obtained from cell signal technology (CST) with the dilution of 1:500 for overnight incubation in cold room. After incubation, cells were washed with PBS and probed with secondary antibody raised against rabbit (Invitrogen 1:2000) which are labeled with FITC for 1 hr at room temperature. Fluorogel containing 4',6-diamidino-2-phenylindole (DAPI) from Electron Microscopy Sciences was used as a counter stain and analyzed using confocal microscopy (Olympus FluoView FV10i).

For F-actin cytoskeleton modification, PCSC (1×10^5) cells were cultured on 8-well chambers and treated with different doses of STL for 48 hrs. After incubation, cells were fixed with 4% para formaldehyde and permeabilised with 0.1% Triton-X-100. Following washes cells were blocked with 5% BSA for 1 hr and incubated with Phalloidin tetramethylrhodamine (TRITC) (1:2000) obtained from Sigma for overnight. After incubation, slides were mounted with fluorogel (Electron microscopy sciences) containing DAPI and fluorescence staining analyzed using confocal microscopy (Olympus FluoView FV10i) [47].

Calcein green was used to determine the iron levels upon treatment with STL. For this, PCSC (1×10^5) were seeded onto 8-well chambers and treated with various doses of STL and incubated at 37°C for 6 hrs. Following incubation, cells were stained with Calcein green (50 µM) and incubated at 37°C for 30 min. After staining, cells were fixed with 4% paraformaldehyde for 15 min and analyzed using confocal microscopy (Olympus FluoView FV10i).

Aldehyde dehydrogenase expression by flow cytometry

PCSC (1×10^6) were seeded onto FBN coated flasks and treated with various concentrations of STL (10, 25 and 50 µM) for 48 hrs. After treatment, live and dead cells were collected and stained with ALDH1 (1:100) tagged with FITC antibody and incubated for 30 min on ice and analyzed using flow cytometry (FACS Calibur, BD Biosciences, Mountain View, CA). Data was quantified using FlowJo software.

Western blot assay

PCSC were seeded at a density of 1×10^6 cells on FBN coated T25 flasks and cultured with

STL (10, 25 and 10 μM) for 48 hrs. Afterwards, the cells were collected using cell scraper and washed with ice cold 1×PBS for 5 min. Subsequently, cell lysis buffer containing protease inhibitor was added and incubated on ice for 5 min. Afterwards, cell lysate was centrifuged for 5 min and supernatant was collected into a fresh tube. Protein concentrations were estimated by Pierce Rapid Gold BCA Protein Assay. A total of 20 μg of protein was resolved on a 10-12% sodium dodecyl sulfate-polyacrylamide gel electrophoresis and then transferred to nitro cellulose membranes (GE Healthcare Life Sciences). Membranes were blocked with 5% skim milk in Tris-buffered saline with Tween-20 (TBST) for 1 hr at room temperature, prior to be incubated with primary rabbit anti-human antibodies against survivin, TCTP, phospho TCTP, cleaved caspase3, cleaved PARP-1, X-linked inhibitor of apoptosis (XIAP), Phospho-Histone H2A.X (pH2A.X), Phospho and total 5'AMP-activated protein kinase (AMPK), Phospho and total p38 MAPK, Phospho p44/42 MAPK (Erk1/2) and total p44/42 MAPK (Erk1/2), TCF8, LEF1, cdc2, phospho Histone H3, Beclin1, Autophagy-related gene (ATG) 5, light chain 3 (LC3) (Cell Signaling Technologies, USA; 1:1000 dilution) and mouse anti-beta actin labeled with HRP (Sigma; 1:50000). Apart from beta actin (Sigma), all the primary antibodies were obtained from CST. Reactive bands were detected by ECL method [47].

Statistical analysis

The Student's t-test was used to compare the treatment and control groups. A *P*-value <0.05 was considered to be statistically significant. Each experiment was repeated for 3 times and data are represented as the mean ± SD unless or otherwise stated.

Results

Anticancer effect of STL on cell growth in PCSC and prostate cancer cells

The anticancer effect of sertraline on cell viability was initially evaluated in PCSC using a standard MTT assay. Compared with control cells (without STL treatment), the cell viability of treated PCSC was inhibited in a dose- and time-dependent manner (**Figure 1A**). The inhibition of cell growth was significant upon treatment with 25 and 50 μM STL for 48 hrs. These results suggested that STL inhibit the cell survival property of PCSC.

In order to identify the cell death mechanism, PCSC were exposed to STL in the presence or absence of antioxidants such as NAC, GSH and catalase. It has been reported that depletion of intra cellular NAC and GSH levels were associated with oxidative stress mechanism. In addition, down regulation of catalase expression reported during oxidative stress. From our data, it can be inferred that NAC, GSH and catalase potently blocked the effect of STL suggesting that oxidative stress could be mediating the effects of STL (**Figure 1B**). This notion is supported by the data presented in **Figure 6** which suggested that STL induced oxidative stress by reducing the level of glutathione and elevating the levels of hydrogen peroxide and lipid peroxidation in PCSC. Furthermore, MTT cell viability assay was performed to identify the role of iron in the cytotoxic effects of STL. Our data revealed that STL exerted synergic effect in the presence of FS and iron chelators such as DFO and DPP44MT (**Figure 1C**). These results indicate that STL disrupts the viability of PCSC by potentially modulating iron homeostasis in PCSC. Further, we also analyzed the anticancer activity of STL on PC3, DU145 and LNCaP prostate cancer cell lines. Cells were treated with various concentration of STL (1-100 μM) and incubated for 48 hrs. **Figure 1D** shows that STL administered to prostate cancer cells resulted in rapid killing in a dose dependent effect with IC_{50} of 10 μM for 48 hrs. As the concentration was increased to 15 μM and above, a significant decline in the viable cells was observed. Dosage above 10 μM exhibited similar effects in these prostate cancer cell lines.

STL inhibits the clonogenic growth and Spheroid formation of PCSC and disrupts the tube formation of HUVEC cells

Cancer stem cells have the ability to form larger colonies from single clone and responsible for tumor growth and progression. We tested the effect of STL on colony formation and spheroid formation abilities of PCSC. Crystal violet staining revealed that STL robustly inhibits the colony formation ability of PCSC with increasing doses (**Figure 2A**, **2B**). Moreover, spheroid formation was visualized using Calcein green

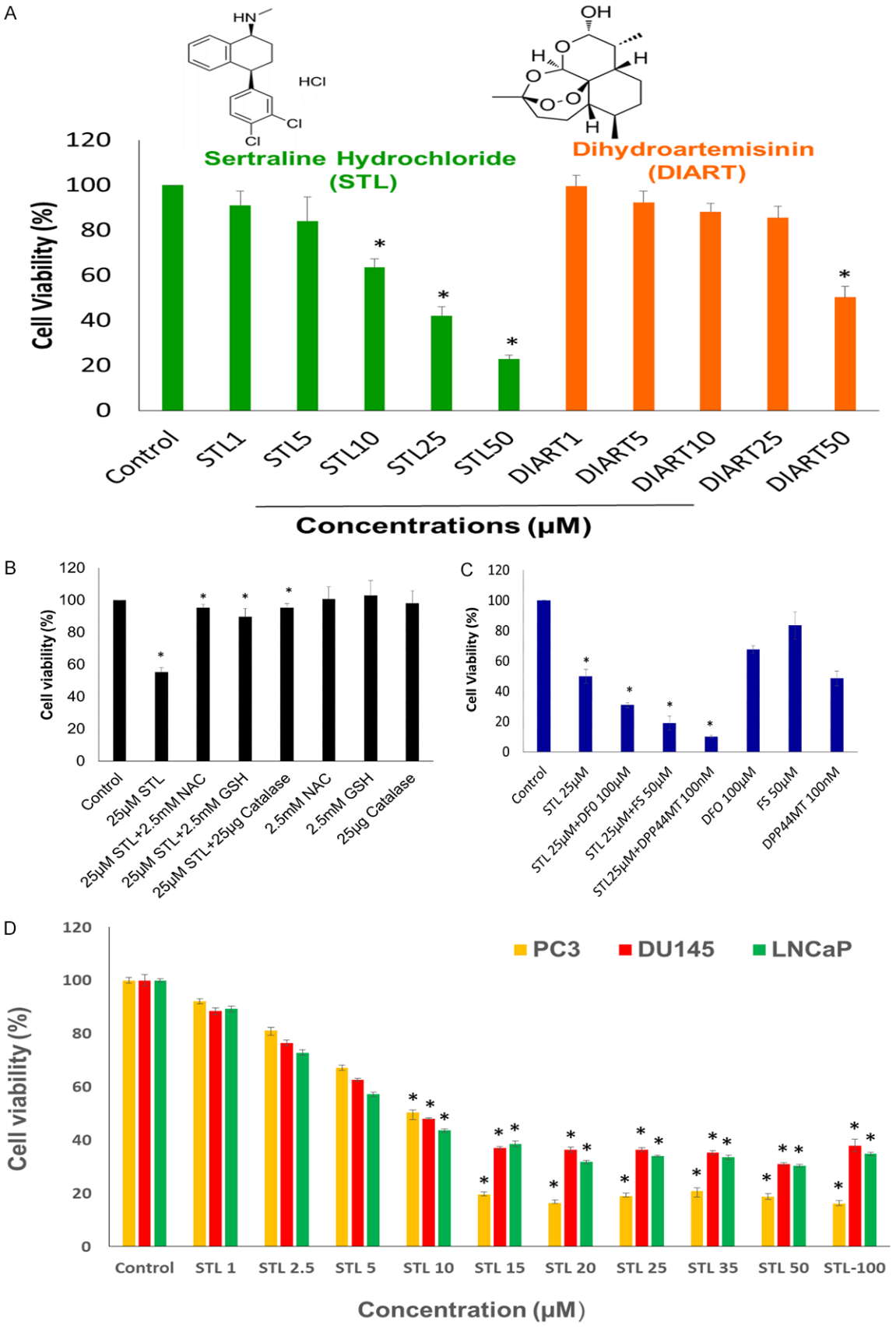
A
HN
HCl
Cl
Cl
OH
H
O
O
O-O
H
H
Sertraline Hydrochloride
(STL)
Dihydroartemisinin
(DIART)
Cell Viability (%)
120
100
80
60
40
20
0
Control
STL1
STL5
STL10
STL25
STL50
DIART1
DIART5
DIART10
DIART25
DIART50
Concentrations (μM)
B
Cell viability (%)
Control
25μM STL
25μM STL+2.5mM NAC
25μM STL+2.5mM GSH
25μM STL+25μg Catalase
2.5mM NAC
2.5mM GSH
25μg Catalase
C
Cell Viability (%)
Control
STL 25μM
STL 25μM+DFO 100μM
STL 25μM+FS 50μM
STL25μM+DPP44MT100nM
DFO 100μM
FS 50μM
DPP44MT 100nM
D
PC3
DU145
LNCaP
Cell viability (%)
Control
STL 1
STL 2.5
STL 5
STL 10
STL 15
STL 20
STL 25
STL 35
STL 50
STL-100
Concentration (μM)

Figure 1. PCSC are more sensitive to STL than DIART in inhibiting cell viability. A. Chemical structure of STL and DIART. MTT cell viability of PCSC was performed following treatment with various doses of STL and DIART for 48 hrs. B. STL mechanism of action, PCSC were treated with STL in presence or absence of antioxidants (NAC, GSH and catalase) for 48 hrs and MTT assay was performed. Antioxidants blocks the effect STL on PCSC. C. Cell viability assay of PCSC treated with STL with or without DFO, FS and DPP44MT. In the presence of above mentioned compounds STL showed synergetic effect in inducing cell death. D. To measure the cytotoxicity effect of STL on PC3, DU145 and LNCaP cells, cells were treated with different concentration of STL (1-100 μM) for 48 hrs. Results showed that STL robustly inhibited the viability of prostate cancer cell lines. Cell viability was monitored by MTT assay. The data shown are representative of one of three independent experiments. Data are means ± SD (n = 3). *P<0.05 compared to control.

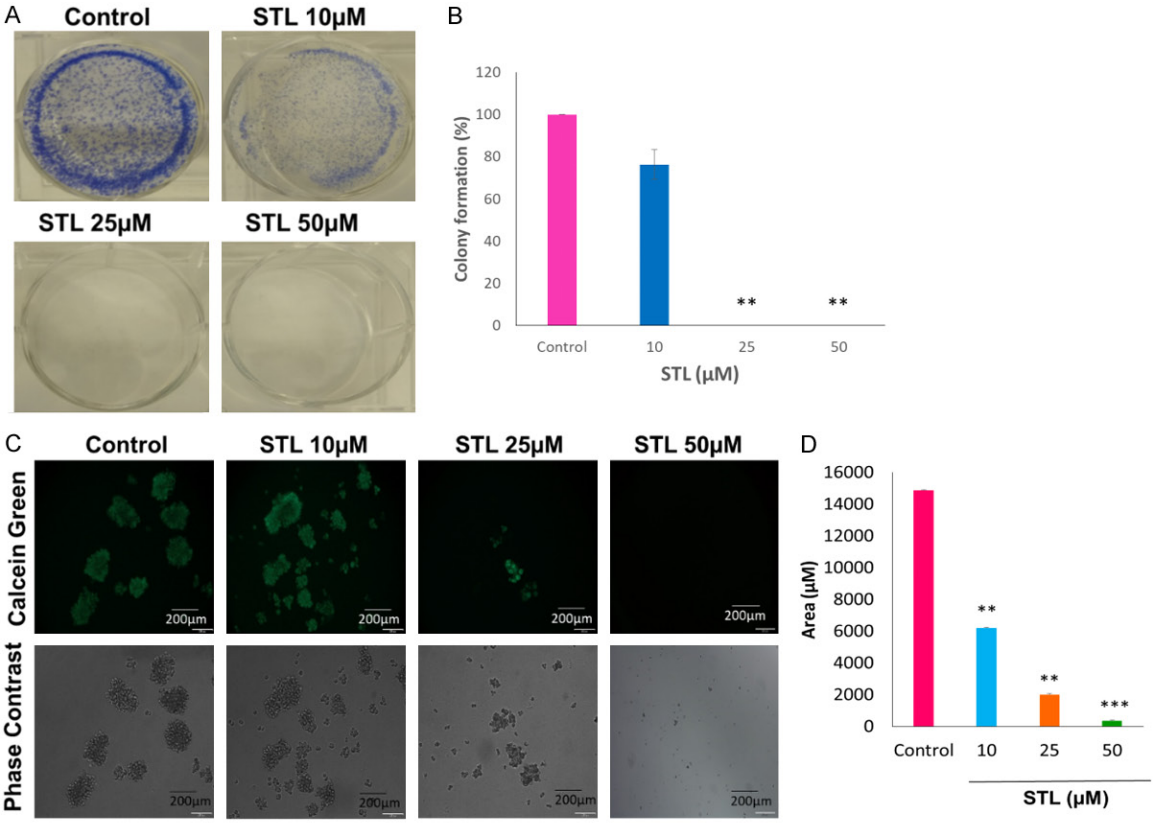

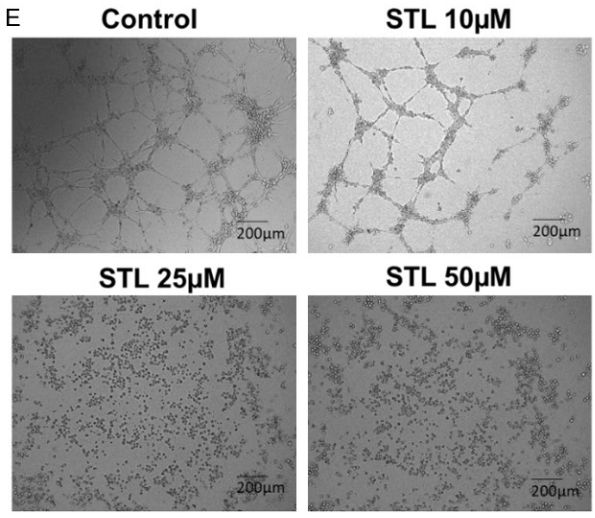

Figure 2. STL inhibits clonogenic potential of PCSC and angiogenesis of HUVEC cells. A, B. PCSC were treated with STL for 2 weeks. Colonies were visualized by crystal violet staining. STL robustly inhibited the colony formation ability of PCSC. C, D. In spheroid assay, PCSC were seeded onto low attachment plates and treated with different doses of STL for 2 weeks. After incubation, cells were stained with Calcein green and measured the size of the spheroid using ImageJ software. Our data revealed that STL inhibited the tumorigenic potential of PCSC. E. In angiogenesis assay, HUVEC cells were cultured on matrigel in the presence or absence of STL for 6 hrs and observed for tube formation. STL significantly inhibited the angiogenic potential of HUVEC tube forming cells. The images were captured using microscopy. Magnification 10×. Scale bar 200 μm. The data shown are representation of one of three independent experiments. Data are means ± SD (n = 3). **P<0.01; ***P<0.001 compared to control.

staining upon treatment with different doses of STL (**Figure 2C**, **2D**). Our data revealed that STL significantly reduced the size of the spheroid formation with increasing doses. From our results, it can be concluded that STL is effective in targeting the clonogenic potential of PCSC. Further, STL inhibited the tube formation of HUVEC endothelial cells (**Figure 2E**) suggesting that STL could also inhibit the angiogenic potential.

STL inhibited migratory properties of PCSC

Cancer stem cells along with tumor cells which detach from primary tumor site and migrate to distant organs such as bone, brain and lymph nodes during metastatic process. To test the effect of STL on migration property, an important characteristic of metastasis, PCSC were treated with different doses of STL followed by wound healing assay and Trans well migration assays were performed. Our wound healing assay data revealed that STL inhibits the migration ability of PCSC. At 50 μM STL, the percentage of gap was higher compared to untreated control (**Figure 3A**, **3B**). Further, we performed Transwell migration assay using Transwell inserts. PCSC were treated with various doses of STL and migrated cells were stained with crystal violet on the bottom side of the insert and bottom side of the 24 well plate. Our data revealed that less number of migrated stained cells were observed in bottom side of the insert (**Figure 3C**, **3D**) and 24 well plate (**Figure 3E**, **3F**) following STL treatment compared to untreated control.

F-actin cytoskeleton plays a major role in cell migration, proliferation and cell division. From our results, it is evident that STL inhibits the F-actin polymerization of PCSC in a dose dependent manner as revealed by Phalloidin staining analysis (**Figure 3G**, **3H**). Significant decrease in F-actin polymerization was observed at 50 μM concentration of STL compared to untreated control. Here, we can conclude that STL is more potent in targeting the migration properties and F-actin cytoskeleton dynamics of PCSC.

STL promotes G_0 arrest and apoptosis induction in PCSC

To determine whether the reduction in cell viability is associated with STL mediated cell death in PCSC, Annexin V-FITC/PI Apoptosis detection kit was used to determine the percentage of apoptotic cell death using flow cytometry. Our dot plots and graphical representations show that STL induced early and late apoptosis upon STL treatment. The percentage of cell death increase with increasing doses. Upon treatment with 25 and 50 μM STL for 48 hrs, apoptosis was significantly increased, compared with that of control PCSC (**Figure 4A**, **4B**). The results showed that anticancer property of STL is via inducing programmed cell death.

Further, we checked on the cell cycle distribution of PCSC upon STL treatment. The cell cycle analysis of STL treated PCSC were analyzed using PI staining by flow cytometry. After 48 hrs of 25 and 50 μM STL treatment, percentage of PCSC in G_0 phase increased in a dose dependent manner. The results indicated that STL hinders with cell cycle progression and impairing PCSC malignant properties (**Figure 4C**, **4D**).

STL induced superoxide generation and hydrogen peroxide formation in PCSC

Next, we determined the ROS levels in PCSC upon STL treatment. Oxidative stress plays an important role in cell death mechanism. To this end, PCSC were treated with various doses of STL and stained with ROS probe H2DCFDA. Fluorescence microscopic images indicated that STL induced the formation of free radical generation with increasing doses (**Figure 5A**, **5B**). Oxidative stress known to affect the mitochondrial membrane potential during cell death mechanism. For this, PCSC were treated with different doses of STL and stained with Mitosox red for superoxide anion and visualized using fluorescence microspore and quantified using flow cytometry. Quantification of fluorescence microscopic images (**Figure 5C**, **5D**) and histograms of flowcytometric analysis (**Figure 5E**, **5F**) show that STL significantly induced superoxide anion formation. Our data indicated that STL induced PCSC cell death mechanism by inducing mitochondrial depolarization.

STL induced hydrogen peroxide formation, lipid peroxidation and depleted the levels of reduced GSH

Next, we determined the effect of STL on hydrogen peroxide, lipid peroxidation and reduced

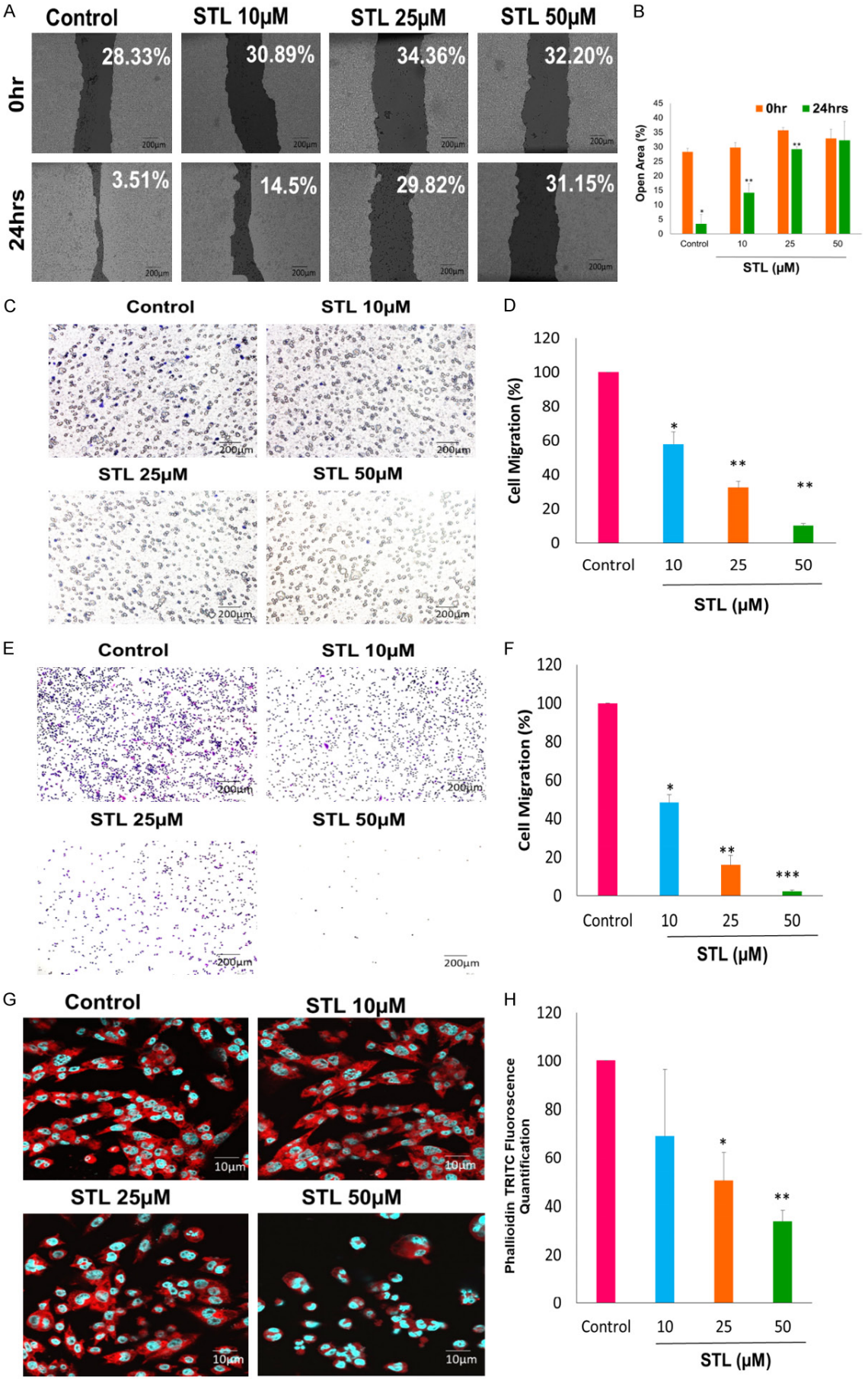
A
Control
STL 10μM
STL 25μM
STL 50μM
0hr
24hrs
28.33%
30.89%
34.36%
32.20%
3.51%
14.5%
29.82%
31.15%
200μm
B
0hr
24hrs
Open Area (%)
Control
10
25
50
STL (μM)
C
Control
STL 10μM
STL 25μM
STL 50μM
200μm
D
Cell Migration (%)
Control
10
25
50
STL (μM)
E
Control
STL 10μM
STL 25μM
STL 50μM
200μm
F
Cell Migration (%)
Control
10
25
50
STL (μM)
G
Control
STL 10μM
STL 25μM
STL 50μM
10μm
H
Phallioidin TRITC Fluoroscence Quantification
Control
10
25
50
STL (μM)

Figure 3. STL inhibits migration properties and actin cytoskeleton of PCSC. A. PCSC were seeded onto 24 well plate and allowed to grow until 100% confluence, scratch was made and cells were allowed to close the wound in presence or absence of STL for 24 hrs and imaged. Magnification 10×. Scale Bar 200 µm. B. T-Scratch quantified results of wound healing. C-F. For Transwell migration assay without matrigel, PCSC were seeded onto Transwell insert with different doses of STL for 24 hrs. Migrated cells were stained with 0.05% crystal violet. Scale bar = 200 µm. Representative images are shown on the left panel, and the statistical graphs on the right panel indicating the average number of cells per field after 24 hrs of STL treatment. (*P<0.05, compared with control). G, H. Confocal images of PCSC treated with STL targets the actin cytoskeleton and promote the cell death with increasing doses. Phalloidin TRITC was used to stain F-actin and DAPI was used to satin nucleus. The percentage of actin expression decreases with increasing doses of STL. Magnification 63×. Scale bar 10 µm. Images showing that STL significantly inhibiting the actin cytoskeleton modification. The data shown are representative of one of three independent experiments. Data are means ± SD (n = 3). *P<0.05; **P<0.01; ***P<0.001 compared to control.

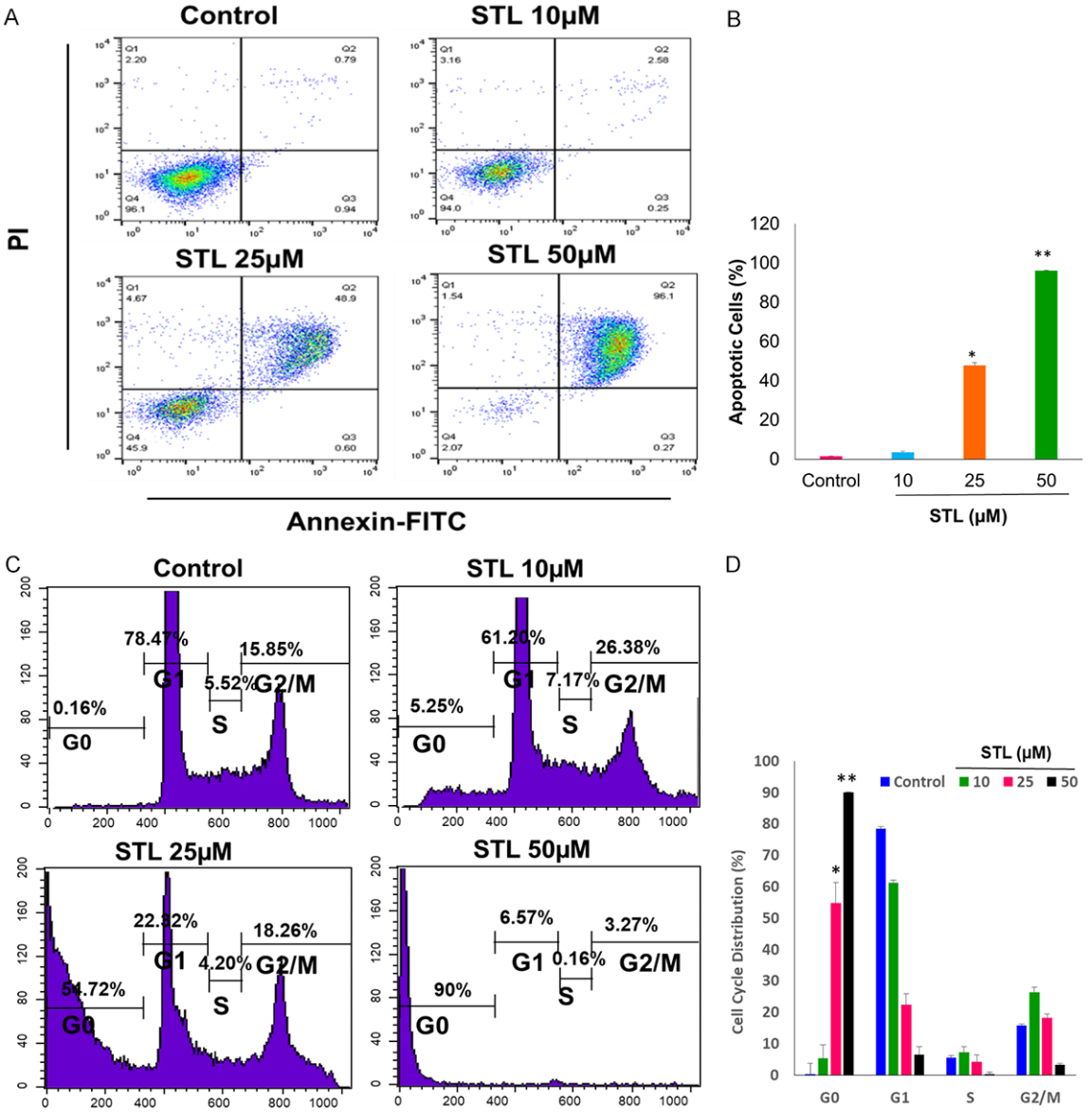

Figure 4. STL induced apoptosis in PCSC by disrupting the cell cycle progression. A, B. The percentage of cell death was determined by Annexin V-FITC/PI flow cytometry. The Annexin V-FITC/PI staining revealed that STL significantly induces cell death by apoptotic mechanism. C, D. Effects on cell cycle profile of PCSC after treatment with STL. Cells were treated with STL for 48 hrs and then fixed with 70% ice cold ethanol, and the DNA content was determined by flow cytometry analysis by PI staining, analyzing 50,000 events per sample. Results showed that majority of cells treated with STL accumulated in G_0 phase which is suggestive of dying cells. The data shown are representation of one of three independent experiments. Data are means ± SD (n = 3). *P<0.05; **P<0.01 compared to control.

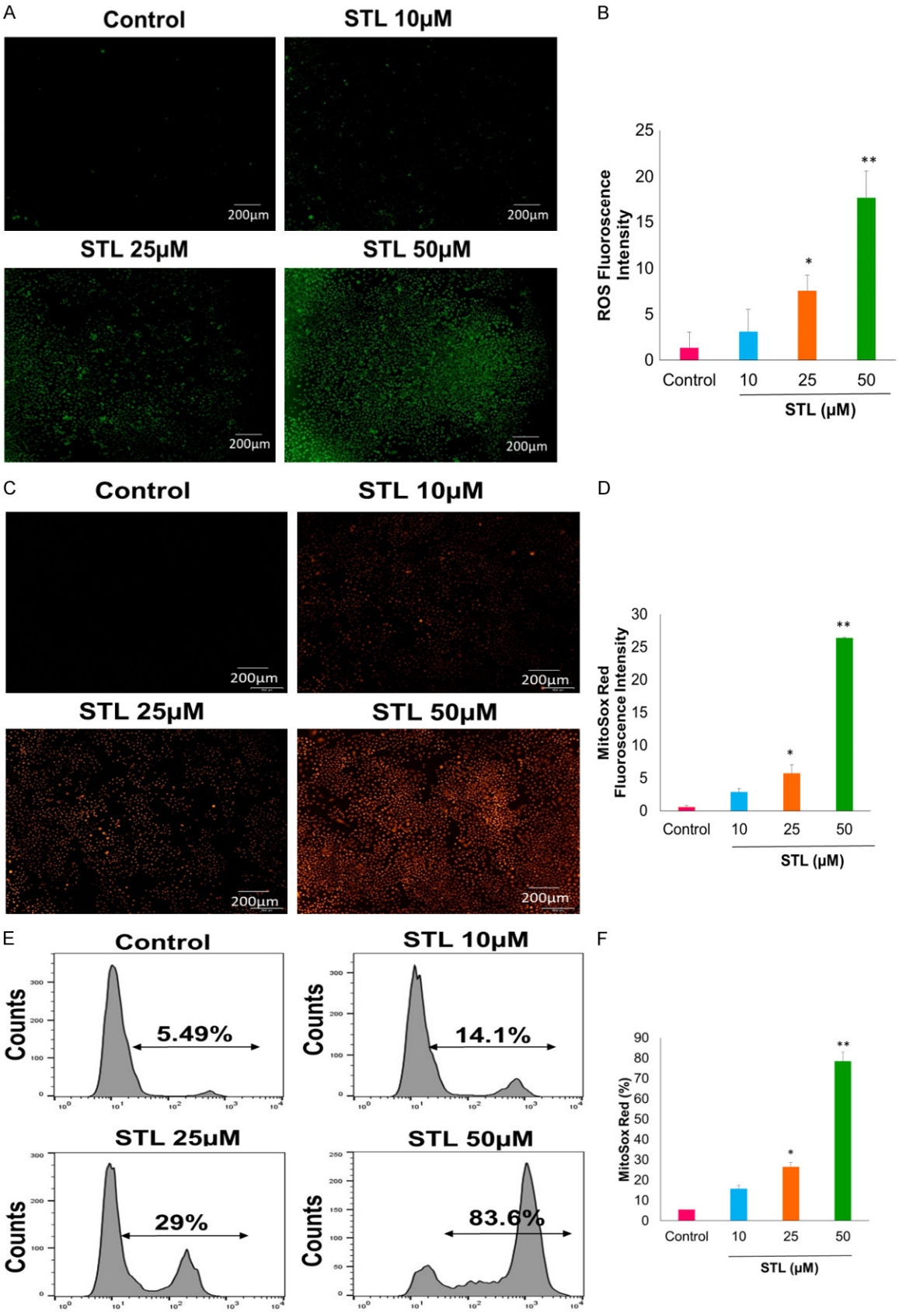
A
Control
STL 10μM
STL 25μM
STL 50μM
200μm
B
ROS Fluoroscence Intensity
25
20
15
10
5
0
**
*
Control
10
25
50
STL (μM)
C
Control
STL 10μM
STL 25μM
STL 50μM
200μm
D
MitoSox Red Fluoroscence Intensity
30
25
20
15
10
5
0
**
*
Control
10
25
50
STL (μM)
E
Control
STL 10μM
STL 25μM
STL 50μM
Counts
5.49%
14.1%
29%
83.6%
F
MitoSox Red (%)
90
80
70
60
50
40
30
20
10
0
**
*
Control
10
25
50
STL (μM)

Figure 5. STL treatment generates reactive oxygen species in PCSC. A-D. PCSC were treated with STL for 6 hrs. PCSC were stained with H2DCFDA probe for ROS (green) and Mitosox Red for superoxide anion production. Fluorescence images of green or red were observed in PCSC with increasing dose of STL suggesting the generation of reactive oxygen species and superoxide anions respectively. Magnification 10×. Scale Bar 200 μm. E, F. Flow cytometric histogram analysis of PCSC treated with STL show increased percentage of mitochondrial superoxide anions with increasing doses of STL. *P<0.05; **P<0.01 compared to control.

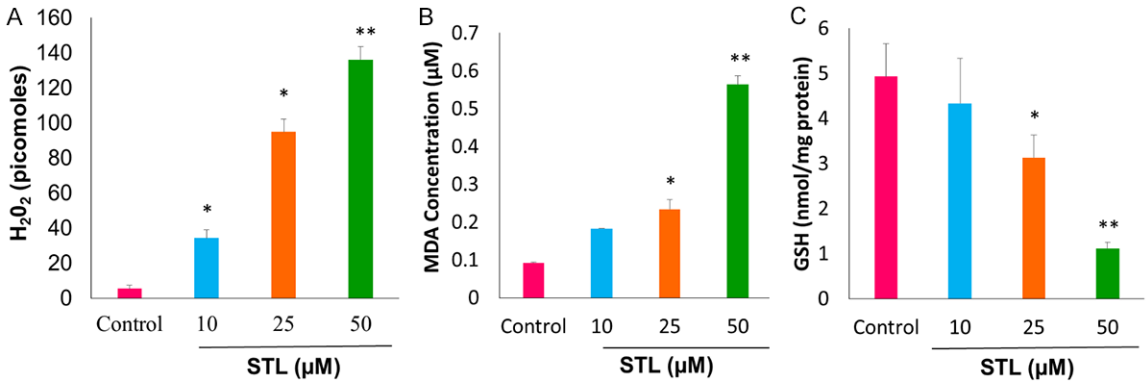

Figure 6. STL treatment elevated the levels of hydrogen peroxide and lipid peroxidation with concomitant reduction of the glutathione levels in PCSC. A. Determination of H_2O_2 levels using hydrogen peroxide assay upon treatment with STL for 6 hrs. Our data suggest that STL induces cell death mechanism by generating hydrogen peroxide levels in PCSC. B. Measurement of lipid peroxidation using TBARS assay of PCSC for 6 hrs which indicates that STL induces lipid peroxidation during cell death mechanism. C. Reduced levels of glutathione upon STL treatment for 6 hrs. The depleted levels of GSH indicates oxidative stress mediated by STL on PCSC. Data are means ± SD (n = 3). *P<0.05; **P<0.01 compared to control.

GSH levels of PCSC. For this, PCSC were treated with different doses of STL and performed the assays as mentioned in methods. STL significantly increased the hydrogen peroxide (**Figure 6A**) and lipid peroxidation (**Figure 6B**) levels whereas glutathione levels were found to be decreased in PCSC (**Figure 6C**).

STL inhibited the expression of stem cell markers of PCSC

Stem cell markers such as ALDH1 and CD44 are essential to maintain stemness of the stem cells. We investigated the alteration of stem cell marker expression upon treatment with STL. To detect the expression of stem cell markers upon treatment with STL in PCSC, the cells were treated with different doses and examined for ALDH1 and CD44 expression levels using confocal microscopy. STL significantly down regulates the ALDH1 (**Figure 7A**, **7B**) and CD44 (**Figure 7E**, **7F**) expression levels with increasing doses. Moreover, our flow cytometry data also revealed that STL significantly down regulate the expression levels of ALDH1 (**Figure 7C**, **7D**). These findings suggest that STL is a potential drug for inhibiting the cancer stem cell properties.

STL induced autophagy and modulates iron levels in PCSC

Autophagy is one of the cell death mechanism along with apoptosis and necrosis. We tested the effect of autophagy cell death mechanism on PCSC upon treatment with STL. PCSC were transfected with LC3 plasmid and treated with different doses of STL for 6 hrs. After treatment cell were analyzed for autophagy using confocal microscope. Our data suggests that PCSC treated with STL leads to autophagy compared to control cells (**Figure 8A**, **8B**). Moreover, we also determined the status of iron levels upon treatment with STL. For this, cells were treated with various doses of STL, stained with calcein and analyzed using confocal microscopy. As calcein fluorescence increased proportionally with higher doses of STL which suggests a decrease in iron pool in PCSC (**Figure 8C**, **8D**). Further studies are warranted to find out the significance of reduced iron levels following antidepressant STL treatment.

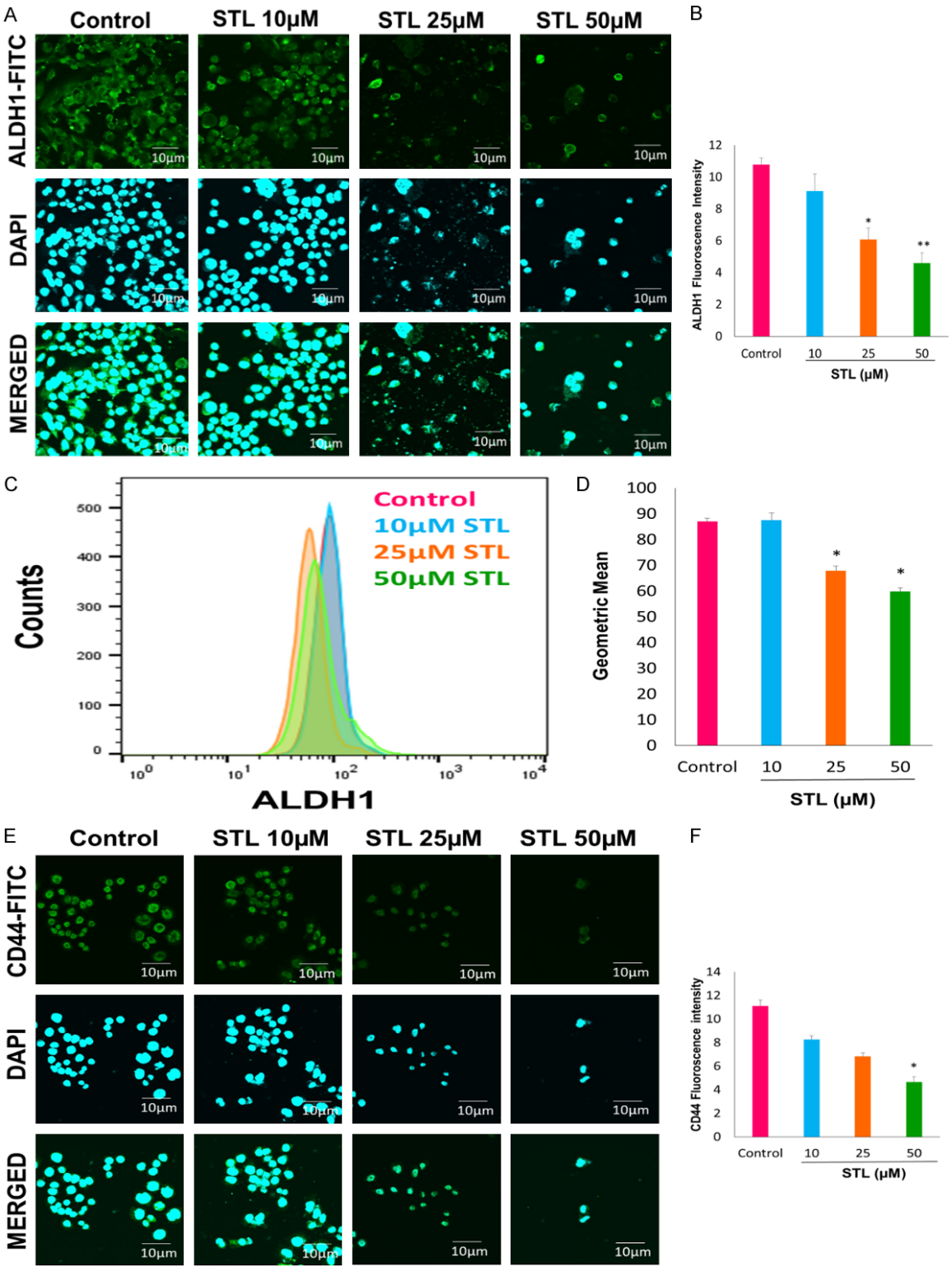

Figure 7. STL down regulates the expression levels of stem cell markers of PCSC. For this, PCSC seeded onto 8-well chambers and treated with various doses of STL for 48 hrs and stained with ALDH1 and CD44, analyzed using confocal microscopy. Image analysis reveal that STL inhibits the expression of both ALDH1 and CD44 in PCSC. A, B. Confocal images of ALDH1 stain and quantification of ALDH1. C, D. Flow cytometric quantification of ALDH1. STL treated PCSC were stained with ALDH1-PE and subjected to flow analysis, and the results of which revealed that STL reduces the surface expression of ALDH1 in PCSC. E, F. Confocal images of CD44 and quantification of CD44. Magnification 60×. Scale bar 10 μm. Our data suggest that STL is more potent in inhibiting stemness of PCSC by targeting ALDH1 and CD44 stem cell markers. *P<0.05; **P<0.01 compared to control.

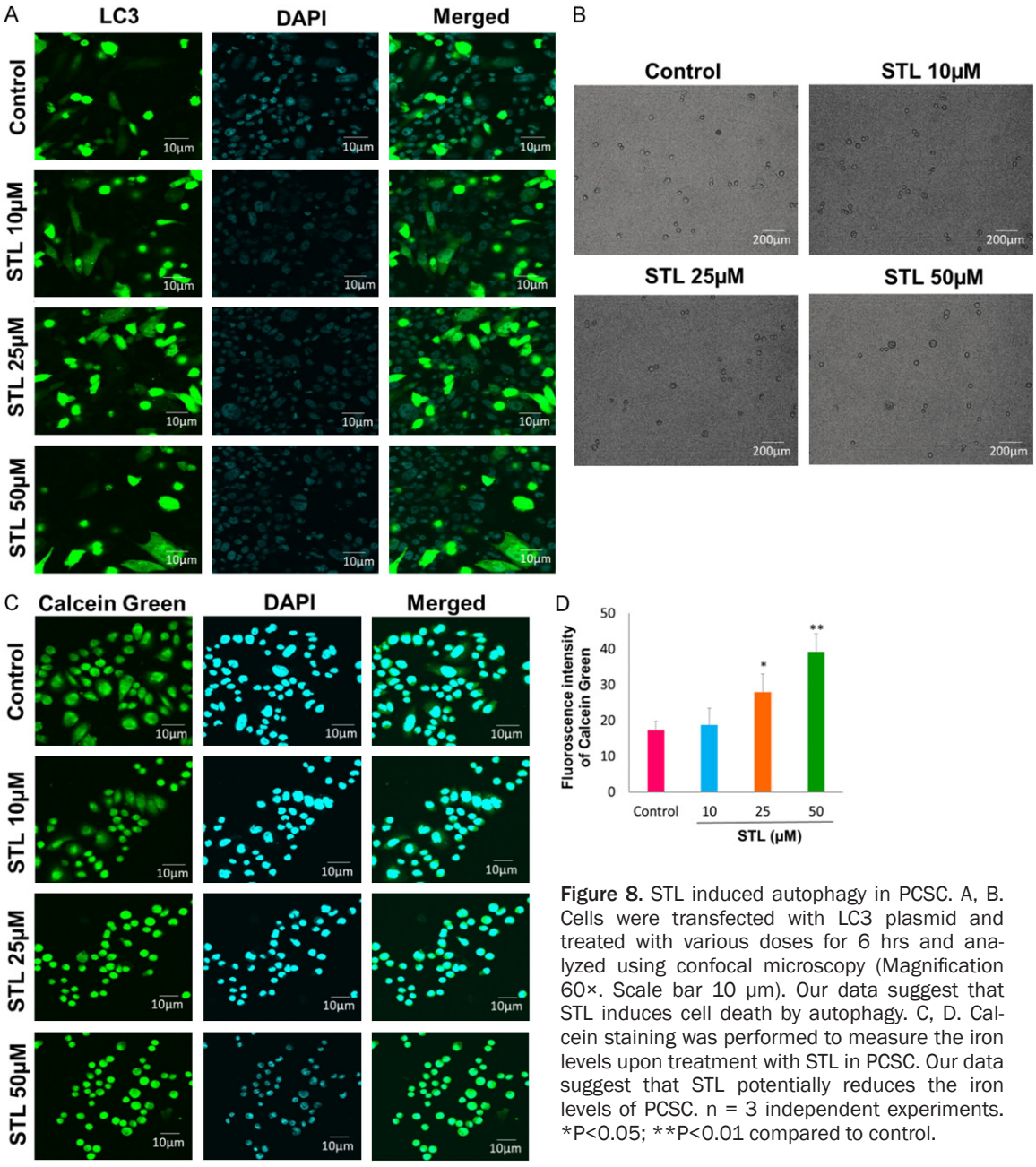

Figure 8. STL induced autophagy in PCSC. A, B. Cells were transfected with LC3 plasmid and treated with various doses for 6 hrs and analyzed using confocal microscopy (Magnification 60×. Scale bar 10 μm). Our data suggest that STL induces cell death by autophagy. C, D. Calcein staining was performed to measure the iron levels upon treatment with STL in PCSC. Our data suggest that STL potentially reduces the iron levels of PCSC. n = 3 independent experiments. *P<0.05; **P<0.01 compared to control.

STL down regulates TCTP and anti-apoptotic marker expression in PCSC

Western blotting demonstrated that antidepressant STL significantly down regulate both phospho and total TCTP expression levels. EMT markers such as TCF8 and LEF1 also down regulated by STL in PCSC. Further, STL inhibited the expression levels of phospho and total P38 mitogen-associated protein kinase (MAPK) and extracellular-signal-regulated kinase (Erk) 1/2 (total and phospho p42/44 MAPK) (**Figure 9A**). Moreover, cleaved PARP1 and cleaved caspase3 levels (**Figure 9A**) were significantly upregulated during apoptosis. Also, STL suppressed the expression levels of anti-apoptotic markers such as survivin, cIAP1 and XIAP in PCSC (**Figure 9B**). In previous studies, TCTP has been shown to be upregulated in most of the cancers including prostate cancer. Therefore, Western blot was performed to identify the expression levels of TCTP and the other markers related to cell death mechanism upon STL treatment in PCSC. Our results indicated that TCTP is the target for STL for elimination of cancer stem cells. Western blot analysis revealed that STL significantly down regulates the total and phospho forms of TCTP during cell death

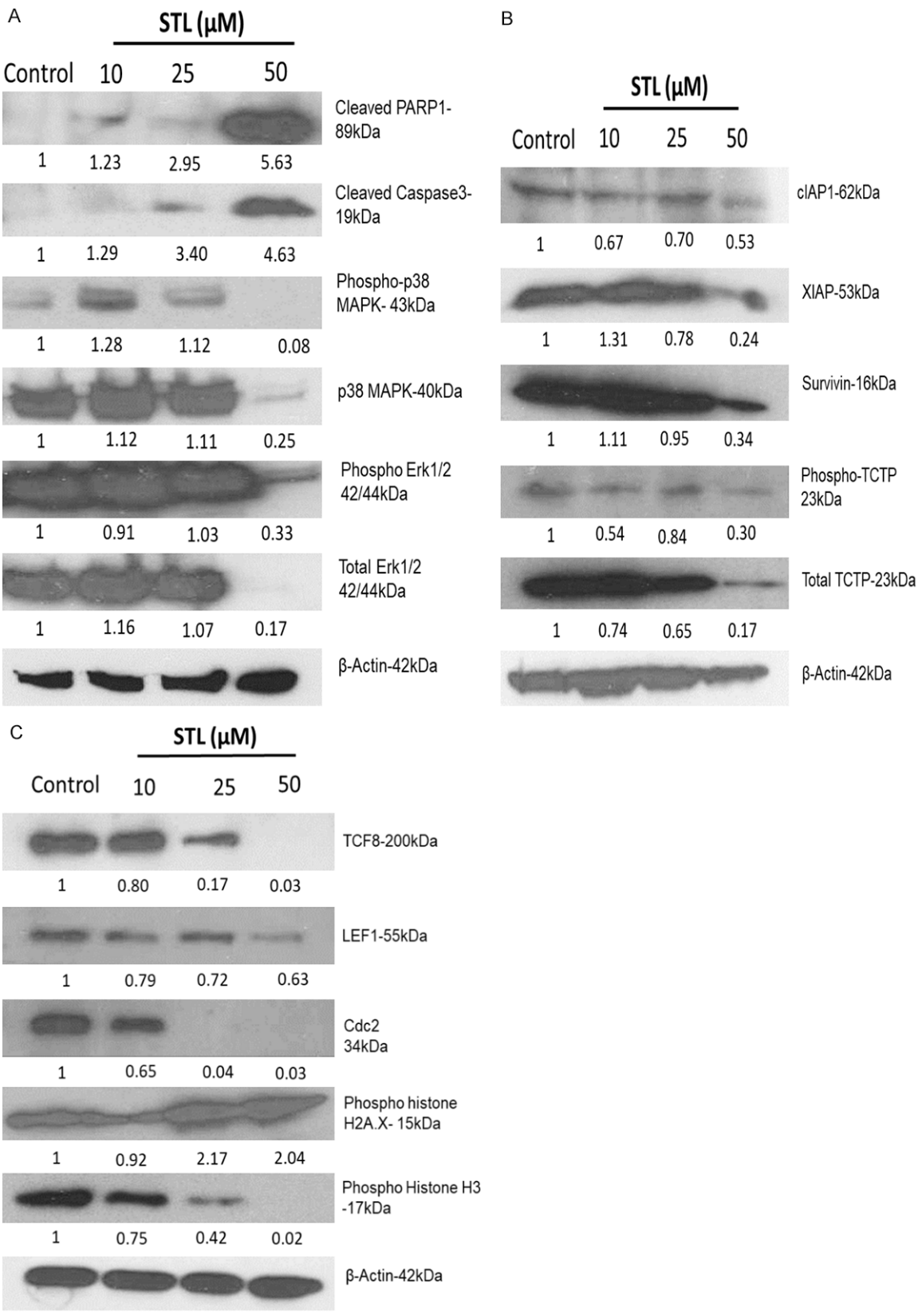
A
STL (μM)
Control 10 25 50
Cleaved PARP1-89kDa
1 1.23 2.95 5.63
Cleaved Caspase3-19kDa
1 1.29 3.40 4.63
Phospho-p38 MAPK- 43kDa
1 1.28 1.12 0.08
p38 MAPK-40kDa
1 1.12 1.11 0.25
Phospho Erk1/2 42/44kDa
1 0.91 1.03 0.33
Total Erk1/2 42/44kDa
1 1.16 1.07 0.17
β-Actin-42kDa
B
STL (μM)
Control 10 25 50
cIAP1-62kDa
1 0.67 0.70 0.53
XIAP-53kDa
1 1.31 0.78 0.24
Survivin-16kDa
1 1.11 0.95 0.34
Phospho-TCTP 23kDa
1 0.54 0.84 0.30
Total TCTP-23kDa
1 0.74 0.65 0.17
β-Actin-42kDa
C
STL (μM)
Control 10 25 50
TCF8-200kDa
1 0.80 0.17 0.03
LEF1-55kDa
1 0.79 0.72 0.63
Cdc2 34kDa
1 0.65 0.04 0.03
Phospho histone H2A.X- 15kDa
1 0.92 2.17 2.04
Phospho Histone H3 -17kDa
1 0.75 0.42 0.02
β-Actin-42kDa

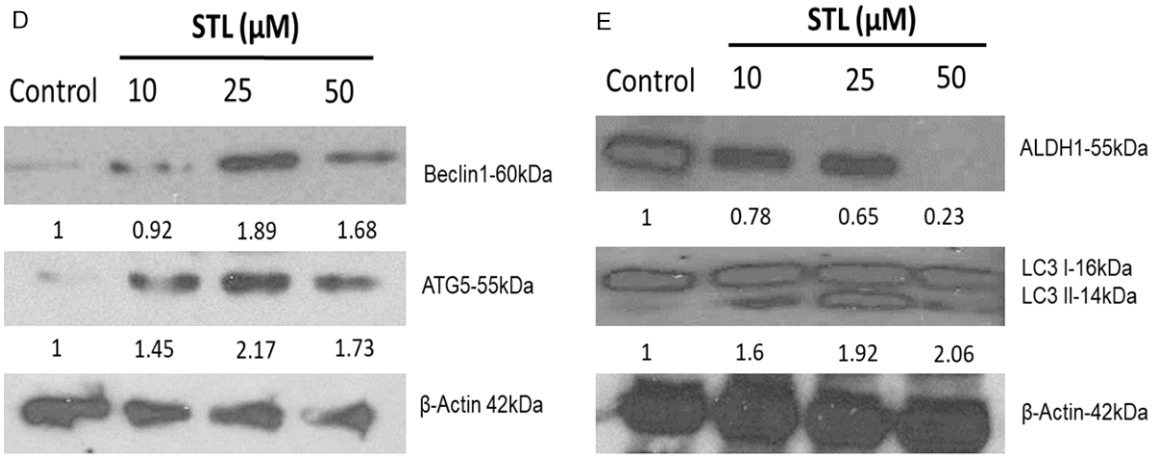

Figure 9. STL modulates various signalling pathways in PCSC. To identify the changes in protein expression levels, PCSC were treated with STL for 48 hrs and cell lysates were subjected to western blot analysis. A. STL treatment promoted cleaved PARP1 and cleaved caspase 3 levels suggesting that it induces apoptosis in PCSC. B. STL concurrently down regulate the expression of anti-apoptotic proteins c-IAP1, XIAP, survivin, TCTP and phospho TCTP. C. PCSC treated with STL showed reduced levels of TCF8, LEF1, cdc2, and phospho Histone H3. On the other hand, pH2A.X was found to be upregulated with STL treatment. D. Exposure of PCSC to STL treatment upregulates the expression of Beclin1 and ATG5 implicating autophagy activation in PCSC. E. STL robustly downregulates the expression of ALDH1 while upregulating LC3 II levels in PCSC. Our data suggest that STL targets multiple signalling pathways to eliminate PCSC. The data represent one of three independent experiments.

(**Figure 9B**). Moreover, STL significantly upregulates the expression levels of autophagy markers such as LC3 (**Figure 9E**), Beclin1 and ATG5 (**Figure 9D**) and down regulates the ALDH1 stem cell marker (ALDH1) (**Figure 9E**) and EMT markers (LEF1 and TCF8) (**Figure 9C**). The expression levels of cdc2 and phospho histone H3 levels were down regulated while phospho histone H2AX was upregulated following STL treatment (**Figure 9C**).

Discussion

PCa, a predominant disease, is considered to be the second most common type of malignant cancer and the leading cause of cancer related mortality in males from United States. PCa has high risk of metastasis and recurrence state following conventional chemotherapy which lead to high mortality rate [49]. Previous studies have reported that cancer stem cell like population is responsible for tumor evolution and progression and as well as resistant to traditional chemotherapeutic drugs [7, 49]. From earlier findings, it has been reported that reducing stress is important for cancer treatment [20, 50, 51]. Further, it was suggested that behavioral stress is associated with PCa progression and development [52]. Our study explored how antidepressant STL targeted the PCSC growth and metastasis. PCSC treated with STL showed significant decrease in cell viability with increasing drug doses and IC_{50} was found to be 25 μM. Our results indicated that antidepressant STL suppresses PCSC growth as well as inhibited the viability of prostate cancer cells (PC3, DU145 and LNCaP). According to present data and the findings from previous reports suggested that STL is a potent inhibitor of cell proliferation in various cancer models [33, 34, 50, 51].

Stress is associated with tumor growth and angiogenesis in ovarian cancer [53]. Our data showed that STL significantly inhibited the growth and angiogenesis of PCSC. These observations suggested that targeting stress in cancer stem cells block the tumorigenic and angiogenic property of cancer cells and could have therapeutic implications. Cancer metastasis is a complex process associated with stress induced cancer cell proliferation, invasion and angiogenesis [54-57]. Our results revealed that STL significantly inhibited the proliferation and migration potential of cancer stem cells from wound healing and transwell migration assays. Stem cell migration is essential for maintaining embryogenesis and to repair the damaged tissues to restore homeostasis. It also plays a major role in cancer development. Previous studies demonstrated that

STL decreases the migration of cancer cells [34]. In consistent with earlier findings, we also found that inhibition of cell migration contributed to cell toxicity of STL on PCSC. Our wound healing assay and transwell migration data revealed that STL significantly inhibited the metastasis ability of PCSC. Expression of EMT markers plays an important role in cancer progression and metastasis. Furthermore, STL inhibited the EMT markers such as TCF8 and LEF1. Collectively our data indicated that STL regulates key signaling molecules involved in cell growth, apoptosis, autophagy, EMT including stem cell program in PCSC.

The cytotoxicity of STL on PCSC was associated with apoptosis. Flow cytometry analysis of Annexin V-FITC/PI dual staining showed that STL induced apoptosis in a dose dependent manner in prostate cancer stem cells. Maximum cell death was observed at 50 μM concentration of STL. The apoptosis induced by STL appears to be associated with free radical generation and dysfunction of mitochondria. Our cell cycle analysis revealed that STL induced G0 arrest in a dose dependent manner. Cell cycle arrest related to the cytotoxicity of STL on prostate cancer stem cells. 10 μM of STL showed minute inhibition of G0 arrest, however 25 and 50 μM of STL showed significant arrest at G_0 phase of the prostate cancer stem cells. Our findings suggested that antidepressant STL induced cell cycle specific mediated cell death.

Oxidative stress play an important role in cell death mechanism of anticancer agents [58]. NAC and GSH are the most effective anticancer compounds that acts as a free radical scavenger. In addition, catalase is an antioxidant enzyme abundantly present in the human body and known to function as a hydrogen peroxide scavenger [47]. The increase in ROS levels induces cell death by lipid peroxidation and deoxyribonucleic acid (DNA) damage by initiating apoptosis. It has been reported that elevated levels of ROS were observed during cell death mechanism. In our study, STL induces free radical formation with increasing doses. In addition, elevated levels of mitochondrial superoxide anion production was observed upon STL treatment. This finding indicated that STL induced cell death by production of reactive oxygen species. Combination study of STL with antioxidants such as NAC, GSH and catalase revealed that STL induces cell death by production of H_2O_2 and other free radical generation. In addition, hydrogen peroxide assay revealed that STL induced apoptosis by formation of hydrogen peroxide in prostate cancer stem cells. The results suggested that oxidative stress plays an important role in STL mediated cell death mechanism.

Next, we performed to check the alterations of markers which are related to cell death mechanism of PCSC upon STL treatment. PARP1 is important for cell survival and is associated with several cellular functions such as apoptosis, DNA replication, transcription, DNA repair and damage (PARP-1, a determinant of cell survival in response to DNA damage). Activation of cleaved PARP1 expression levels were associated with DNA damage and apoptosis [47]. Mediation of PARP1-dependent cell death by apoptosis-inducing factor. Our western blot analysis showed that STL induced cleaved PARP1 activation with increasing doses during apoptosis which correlated with our earlier findings.

Autophagy is one of the important cell death mechanism which is upregulated during stress conditions induced by most of the chemotherapeutic drugs [59]. In our study, we showed that STL induced autophagy of PCSC by upregulating the autophagy markers such as LC3-II, Beclin1 and ATG-5. Earlier reports also suggested that STL induce autophagy in acute myeloid leukemia [30] and retinal pigmented cells [60].

Iron is an important metal for almost all biological systems [61]. The regulation of iron metabolism is important for physiological functions. Imbalance in iron metabolism leads to cell death by generating iron mediated ROS levels [62]. From our study, we observed that STL treatment significantly altered the iron levels, which may have a role in cell death of PCSC. Further studies are required to clarify the role of cellular iron in STL-mediated anti-PCSC effects.

Stem cell markers are responsible for self-renewal and progression of normal and cancer stem cells. ALDH1 expression is associated with chemo resistance and cancer stem cell survival [63]. The expression of ALDH1 plays an important role in formation of cancer stem cells and epithelial to mesenchymal transition [64].

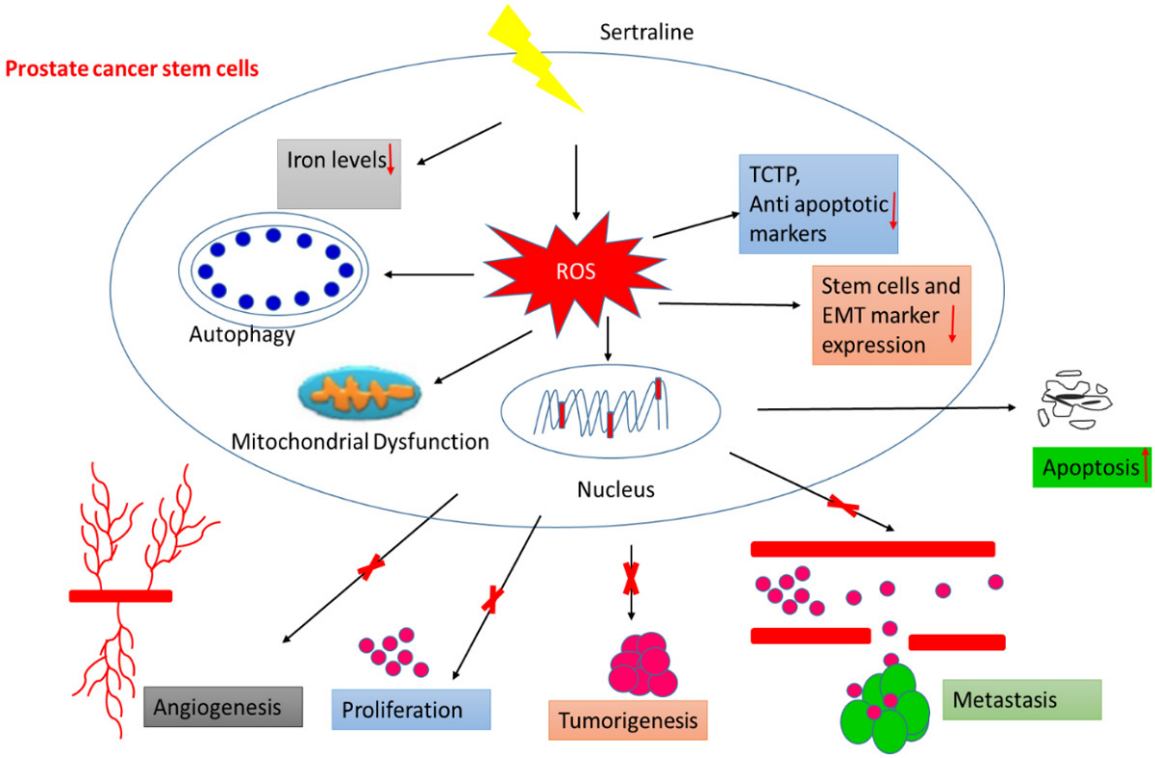

Figure 10. Schematic mechanism of STL targeting PCSC.

Our study show that STL induces the cell death of PCSC by significant down regulation of ALDH1 expression.

Western blot analysis also revealed that activation of cleaved caspase3 following STL treatment. From our earlier reports, activation of caspase cascade was observed during apoptosis. TCTP plays an important role in tumor progression and metastasis. It is also known to induce epithelial to mesenchymal transition (EMT) in lung cancer models. TCTP knock down have been shown to impair the tumor progression and metastasis [34, 36]. Previously we have shown that silencing TCTP expression using siRNA in LNCaP prostate cancer cells leads to apoptotic cell death [67]. A follow up study has shown that knock down of TCTP by antisense oligonucleotides also results in apoptosis of prostate cancer cells [68]. Our western blot analysis revealed that STL significantly down regulates the expression levels of phospho and total TCTP, which is correlated with the previous findings of STL in melanoma treatment [34, 36]. The overall anti-PCSC targeting mechanisms of STL is summarized in **Figure 10**. Our results suggests that TCTP is an effective therapeutic target for treating PCa by targeting PCSC with STL.

In conclusion, our results demonstrate that STL effectively targets PCSC by inducing oxidative stress and promoting cell death via dual activation of apoptosis and autophagy process. In particular, STL down regulating the expression of stem cell markers, EMT markers and anti-apoptotic proteins including TCTP appears to be the underlying mechanism of STL in targeting PCSC. Further preclinical investigations are essential in order to characterize the potential usefulness of STL in treating PCa patients.

Acknowledgements

This study was partly supported by funding received from NIH, United States (R03 CA21-2890, R03 CA227218, and R03 CA230829), William E. McElroy Foundation, and Brovember Inc. Rockford.

Disclosure of conflict of interest

None.

Abbreviations

H2DCFDA, 2',7'-dichlorodihydrofluorescein diacetate; MTT, 3-(4,5-dimethylthiazol-2-yl)-2,5-di-

phenyl tetrazolium bromide; DPP44MT, 4,4 dimethyl-3thiosemicarbazone; DAPI, 4',6-diamidino-2-phenylindole; AMPK, 5'AMP-activated protein kinase; ALDH1, Aldehyde dehydrogenase 1; ATG, Autophagy-related gene; BSA, Bovine serum albumin; cIAP1, Cellular Inhibitor of Apoptosis Protein 1; CD, Cluster of differentiation; DFO, Deferoxamine; DNA, Deoxyribonucleic acid; DIART, Dihydroartimesinin; DTNB, 5,5'-dithio-bis-2-(nitrobenzoic acid); ECL, Enhanced Chemiluminescence; EMT, Epithelial to mesenchymal transition; Erk, Extracellular-signal-regulated kinase; FACS, Fluorescence-activated cell sorting; FS, Ferrostatin; FBN, Fibronectin; FITC, Fluorescein isothiocyanate; GSH, Glutathione; hrs, Hours; H_2O_2, Hydrogen peroxide; LPO, Lipid peroxidation; LC3, Light chain 3; LEF1, Lymphoid enhancer-binding factor-1; MDA, Malondialdehyde; mTOR, Mammalian target of rapamycin; μM, Micromole; MAPK, Microtubule associated protein kinase; min, Minutes; NAC, N-acetyl cysteine; PBS, Phosphate buffer saline; pH2AX, Phospho-Histone H2AX; PARP-1, Poly [ADP-ribose] polymerase 1; PI, Propidium iodide; PCa, Prostate cancer; PCSC, Prostate cancer stem cells; ROS, Reactive oxygen species; SSRI, Serotonin uptake inhibitors; STL, Sertraline; SDS, Sodium dodecyl sulphate; TRITC, Tetramethylrhodamine; TBARS, Thiobarbutiric acid reactive species assay; TCF8, Transcription factor 8; TCTP, Translationally controlled tumour protein; TBS, Tris-buffered saline; TBST, Tris-buffered saline with Tween 20; XIAP, X-linked inhibitor of apoptosis.

Address correspondence to: Dr. Gnanasekar Munirathinam, Department of Biomedical Sciences, University of Illinois College of Medicine, 1601 Parkview Avenue, Rockford 61107, IL, USA. Tel: 815-395-5773; E-mail: mgnanas@uic.edu

References

[1] Siegel RL, Miller KD and Jemal A. Cancer statistics, 2019. CA Cancer J Clin 2019; 69: 7-34.

[2] Stabile A, Orczyk C, Hosking-Jervis F, Giganti F, Arya M, Hindley RG, Dickinson L, Allen C, Punwani S, Jameson C and Freeman A. Medium-term oncological outcomes in a large cohort of men treated with either focal or hemi-ablation using high-intensity focused ultrasonography for primary localized prostate cancer. BJU Int 2019; 124: 431-40.

[3] Dini V, Belli M and Tabocchini MA. Targeting cancer stem cells: protons versus photons. Br J Radiol 2020; 93: 20190225.

[4] Sohn HM, Kim B, Park M, Ko YJ, Moon YH, Sun JM, Jeong BC, Kim YW and Lim W. Effect of CD133 overexpression on bone metastasis in prostate cancer cell line LNCaP. Oncol Lett 2019; 18: 1189-98.

[5] Hung KF, Yang T and Kao SY. Cancer stem cell theory: are we moving past the mist? J Chin Med Assoc 2019; 82: 814-8.

[6] Dragu DL, Necula LG, Bleotu C, Diaconu CC and Chivu-Economescu M. Therapies targeting cancer stem cells: current trends and future challenges. World J Stem Cells 2015; 26: 1185.

[7] Hu Y and Fu L. Targeting cancer stem cells: a new therapy to cure cancer patients. Am J Cancer Res 2012; 2: 340.

[8] Wang T, Narayanaswamy R, Ren H and Torchilin VP. Combination therapy targeting both cancer stem-like cells and bulk tumor cells for improved efficacy of breast cancer treatment. Cancer Biol Ther 2016; 17: 698-707.

[9] Shibata M and Hoque MO. Targeting cancer stem cells: a strategy for effective eradication of cancer. Cancers 2019; 11: 732.

[10] Sapolsky RM. Stress and the brain: individual variability and the inverted-U. Nat Neurosci 2015; 18: 1344.

[11] Schmidt C and Kraft K. Beta-endorphin and catecholamine concentrations during chronic and acute stress in intensive care patients. Eur J Med Res 1996; 1: 528-32.

[12] Hughes MM, Connor TJ and Harkin A. Stress-related immune markers in depression: implications for treatment. Int J Neuropsychopharmacol 2016; 1; 19-6.

[13] Spiegel, D. Cancer and depression. Br J Psychiatry Suppl 1996; 30: 109-16.

[14] Chida Y, Schrempft S and Steptoe A. A novel religious/spiritual group psychotherapy reduces depressive symptoms in a randomized clinical trial. J Relig Health 2016; 55: 1495-506.

[15] Satin JR, Linden W and Phillips MJ. Depression as a predictor of disease progression and mortality in cancer patients: a meta-analysis. Cancer 2009; 115: 5349-61.

[16] Pinquart M and Duberstein PR. Depression and cancer mortality: a meta-analysis. Psychol Med 2010; 40: 1797-810.

[17] Powell ND, Tarr AJ and Sheridan JF. Psychosocial stress and inflammation in cancer. Brain Behav Immun 2013; 30 Suppl: S41-7.

[18] Andersen BL, Kiecolt-Glaser JK and Glaser R. A biobehavioral model of cancer stress and disease course. Am Psychol 1994; 49: 389.

[19] Moreno-Smith M, Lutgendorf SK and Sood AK. Impact of stress on cancer metastasis. Future Oncol 2010; 6: 1863-81.

[20] Chen Z, Zhang P, Xu Y, Yan J, Liu Z, Lau WB, Lau B, Li Y, Zhao X, Wei Y and Zhou S. Surgical

stress and cancer progression: the twisted tango. Mol Cancer 2019; 18: 132.
[21] Steplewski Z, Goldman PR and Vogel WH. Effect of housing stress on the formation and development of tumors in rats. Cancer Lett 1987; 34: 257-61.
[22] Geddes JR and Cipriani A. 2004. Selective serotonin reuptake inhibitors. BMJ 2009; 329: 809-10.
[23] Ostuzzi G, Matcham F, Dauchy S, Barbui C and Hotopf M. Antidepressants for the treatment of depression in people with cancer. Cochrane Database Syst Rev 2018; 4: CD011006.
[24] Fiedorowicz JG and Swartz KL. The role of monoamine oxidase inhibitors in current psychiatric practice. J Psychiatr Pract 2004; 10: 239.
[25] Cipriani A, Purgato M, Furukawa TA, Trespidi C, Imperadore G, Signoretti A, Churchill R, Watanabe N and Barbui C. Citalopram versus other anti-depressive agents for depression. Cochrane Database Syst Rev 2012; 7: CD006534.
[26] Anderson IM, Nutt DJ and Deakin JF. Evidence-based guidelines for treating depressive disorders with antidepressants: a revision of the 1993 British association for psychopharmacology guidelines. J Psychopharmacol 2000; 14: 3-20.
[27] Cloonan SM, Drozgowska A, Fayne D and Williams DC. The antidepressants maprotiline and fluoxetine have potent selective antiproliferative effects against Burkitt lymphoma independently of the norepinephrine and serotonin transporters. Leuk Lymphoma 2010; 51: 523-39.
[28] Levkovitz Y, Gil-Ad I, Zeldich E, Dayag M and Weizman A. Differential induction of apoptosis by antidepressants in glioma and neuroblastoma cell lines. J Mol Neurosci 2005; 27: 29-42.
[29] Wang Y, Hilton BA, Cui K and Zhu MY. Effects of antidepressants on DSP4/CPT-induced DNA damage response in neuroblastoma SH-SY5Y cells. Neurotox Res 2015; 28: 154-70.
[30] Xia Z, Bergstrand A, DePierre JW and Nässberger L. The antidepressants imipramine, clomipramine, and citalopram induce apoptosis in human acute myeloid leukemia HL-60 cells via caspase-3 activation. J Biochem Mol Toxicol 1999; 13: 338-47.
[31] Grygier B, Arteta B, Kubera M, Basta-Kaim A, Budziszewska B, Leśkiewicz M, Curzytek K, Duda W, Lasoń W and Maes M. Inhibitory effect of antidepressants on B16F10 melanoma tumor growth. Pharmacol Rep 2013; 65: 672-81.
[32] Kurita JI, Hirao Y, Nakano H, Fukunishi Y and Nishimura Y. Sertraline, chlorprothixene, and chlorpromazine characteristically interact with the REST-binding site of the corepressor mSin3, showing medulloblastoma cell growth inhibitory activities. Sci Rep 2018; 8: 13763.
[33] Di Rosso ME, Sterle HA, Cremaschi GA and Genaro AM. Beneficial effect of fluoxetine and sertraline on chronic stress-induced tumor growth and cell dissemination in a mouse model of lymphoma: crucial role of antitumor immunity. Front Immunol 2018; 9: 1341.
[34] Boia-Ferreira M, Basílio AB, Hamasaki AE, Matsubara FH, Appel MH, Da Costa CR, Amson R, Telerman A, Chaim OM, Veiga SS and Senff-Ribeiro A. TCTP as a therapeutic target in melanoma treatment. Br J Cancer 2017; 117: 656-65.
[35] Amson R, Auclair C, André F, Karp J and Telerman A. Targeting TCTP with sertraline and thioridazine in cancer treatment. Results Probl Cell Differ 2017; 64: 283-290.
[36] Amson R, Pece S, Lespagnol A, Vyas R, Mazzarol G, Tosoni D, Colaluca I, Viale G, Rodrigues-Ferreira S, Wynendaele J and Chaloin O. Reciprocal repression between P53 and TCTP. Nat Med 2012; 18: 91.
[37] Kaarbø M, Storm ML, Qu S, Wæhre H, Risberg B, Danielsen HE and Saatcioglu F. TCTP is an androgen-regulated gene implicated in prostate cancer. PLoS One 2013; 8; 7.
[38] Baylot V, Katsogiannou M, Andrieu C, Taieb D, Acunzo J, Giusiano S, Fazli L, Gleave M, Garrido C and Rocchi P. Targeting TCTP as a new therapeutic strategy in castration-resistant prostate cancer. Mol Ther 2012; 20: 2244-56.
[39] Tuynder M, Fiucci G, Prieur S, Lespagnol A, Géant A, Beaucourt S, Duflaut D, Besse S, Susini L, Cavarelli J and Moras D. Translationally controlled tumor protein is a target of tumor reversion. Proc Natl Acad Sci U S A 2004; 101: 15364-9.
[40] Phanthaphol N, Techasen A, Loilome W, Thongchot S, Thanan R, Sungkhamanon S, Khuntikeo N, Yongvanit P and Namwat N. Upregulation of TCTP is associated with cholangiocarcinoma progression and metastasis. Oncol Lett 2017; 14: 5973-5979.
[41] Phanthaphol N, Techasen A, Loilome W, Thongchot S, Thanan R, Sungkhamanon S, Khuntikeo N, Yongvanit P and Namwat N. Upregulation of TCTP is associated with cholangiocarcinoma progression and metastasis. Oncol Lett 2017; 14: 5973-9.
[42] Sun R, Lu X, Gong L and Jin F. TcTP promotes epithelial-mesenchymal transition in lung adenocarcinoma. Onco Targets Ther 2019; 12: 1641.
[43] Bae SY, Kim HJ, Lee KJ and Lee K. Translationally controlled tumor protein induces epithelial to mesenchymal transition and promotes cell migration, invasion and metastasis. Sci Rep 2015; 5: 8061.

[44] Jiang C, Li S, Li Y and Bai Y. Anticancer effects of dihydroartemisinin on human esophageal cancer cells in vivo. Anal cell pathol (Amst) 2018; 2018: 8759745.
[45] Lucibello M, Adanti S, Antelmi E, Dezi D, Ciafrè S, Carcangiu ML, Zonfrillo M, Nicotera G, Sica L, De Braud F and Pierimarchi P. Phospho-TCTP as a therapeutic target of Dihydroartemisinin for aggressive breast cancer cells. Oncotarget 2015; 6: 5275.
[46] Morrissey C, Gallis B, Solazzi JW, Kim BJ, Gulati R, Vakar-Lopez F, Goodlett DR, Vessella RL and Sasaki T. Effect of artemisinin derivatives on apoptosis and cell cycle in prostate cancer cells. Anticancer Drugs 2010; 21: 423.
[47] Chinnapaka S, Zheng G, Chen A and Munirathinam G. Nitro aspirin (NCX4040) induces apoptosis in PC3 metastatic prostate cancer cells via hydrogen peroxide (H2O2)-mediated oxidative stress. Free Radic Biol Med 2019; 143: 494-509.
[48] Singh N, Deeba Zaidi HS, Sharma R and Balapure AK. Polyphenols sensitization potentiates susceptibility of MCF-7 and MDA MB-231 cells to Centchroman. PLoS One 2012; 7: 6.
[49] Gilbert CA and Ross AH. Cancer stem cells: cell culture, markers, and targets for new therapies. J Cell Biochem 2009; 108: 1031-8.
[50] Gil-Ad I, Zolokov A, Lomnitski L, Taler M, Bar M, Luria D, Ram E and Weizman A. Evaluation of the potential anti-cancer activity of the antidepressant sertraline in human colon cancer cell lines and in colorectal cancer-xenografted mice. Int J Oncol 2008; 33: 277-86.
[51] Li XJ, Dai ZY, Zhu BY, Zhen JP, Yang WF and Li DQ. Effects of sertraline on executive function and quality of life in patients with advanced cancer. Med Sci Monit 2014; 20: 1267.
[52] Hassan S, Karpova Y, Baiz D, Yancey D, Pullikuth A, Flores A, Register T, Cline JM, D'Agostino R, Danial N and Datta SR. Behavioral stress accelerates prostate cancer development in mice. J Clin Invest 2013; 25: 123.
[53] Thaker PH, Han LY, Kamat AA, Arevalo JM, Takahashi R, Lu C, Jennings NB, Armaiz-Pena G, Bankson JA, Ravoori M and Merritt WM. Chronic stress promotes tumor growth and angiogenesis in a mouse model of ovarian carcinoma. Nat Med 2006; 12: 939-44.
[54] Fisher ER and Fisher B. Recent observations on concepts of metastasis. Arch Pathol 1967; 83: 321-4.
[55] Yang EV, Sood AK, Chen M, Li Y, Eubank TD, Marsh CB, Jewell S, Flavahan NA, Morrison C, Yeh PE and Lemeshow S. Norepinephrine upregulates the expression of vascular endothelial growth factor, matrix metalloproteinase (MMP)-2, and MMP-9 in nasopharyngeal carcinoma tumor cells. Cancer Res 2006; 66: 10357-64.
[56] Masur K, Niggemann B, Zanker KS and Entschladen F. Norepinephrine-induced migration of SW 480 colon carcinoma cells is inhibited by β-blockers. Cancer Res 2001; 61: 2866-9.
[57] Drell T, Joseph J, Lang K, Niggemann B, Zaenker KS and Entschladen F. Effects of neurotransmitters on the chemokinesis and chemotaxis of MDA-MB-468 human breast carcinoma cells. Breast Cancer Res Treat 2003; 80: 63-70.
[58] Prabha PS, Das UN, Koratkar R, Sagar PS and Ramesh G. Free radical generation, lipid peroxidation and essential fatty acids in uncontrolled essential hypertension. Prostaglandins Leukot Essent Fatty Acids 1990; 41: 27-33.
[59] Fulda S. Autophagy in cancer therapy. Front Oncol 2017; 7; 128.
[60] Kim ES, Shin JH, Park SJ, Jo YK, Kim JS, Kang IH, Nam JB, Chung DY, Cho Y, Lee EH and Chang JW. Inhibition of autophagy suppresses sertraline-mediated primary ciliogenesis in retinal pigment epithelium cells. PLoS One 2015; 10: 2.
[61] Richardson DR and Ponka P. The molecular mechanisms of the metabolism and transport of iron in normal and neoplastic cells. Biochim Et Biophys Acta 1997; 1331: 1-40.
[62] Stohs SJ and Bagchi D. Oxidative mechanisms in the toxicity of metal ions. Free Radic Biol Med 1995; 18: 321-36.
[63] Clark DW and Palle K. Aldehyde dehydrogenases in cancer stem cells: potential as therapeutic targets. Ann Transl Med 2016; 4: 24.
[64] Wang J, Nikhil K, Viccaro K, Chang L, White J and Shah K. Phosphorylation-dependent regulation of ALDH1A1 by Aurora kinase A: insights on their synergistic relationship in pancreatic cancer. BMC Biol 2017; 15: 10.
[65] Sarveswaran S, Varma NR, Morisetty S and Ghosh J. Inhibition of 5-lipoxygenase downregulates stemness and kills prostate cancer stem cells by triggering apoptosis via activation of c-Jun N-terminal kinase. Oncotarget 2019; 10: 424.
[66] Yang DR, Ding XF, Luo J, Shan YX, Wang R, Lin SJ, Li G, Huang CK, Zhu J, Chen Y and Lee SO. Increased chemosensitivity via targeting testicular nuclear receptor 4 (TR4)-Oct4-interleukin 1 receptor antagonist (IL1Ra) axis in prostate cancer CD133+ stem/progenitor cells to battle prostate cancer. J Biol Chem 2013; 288: 16476-83.

[67] Gnanasekar M, Thirugnanam S, Zheng G, Chen A and Ramaswamy K. Gene silencing of translationally controlled tumor protein (TCTP) by siRNA inhibits cell growth and induces apoptosis of human prostate cancer cells. Int J Oncol 2009; 34: 1241-6.

[68] Baylot V, Katsogiannou M, Andrieu C, Taieb D, Acunzo J, Giusiano S, Fazli L, Gleave M, Garrido C and Rocchi P. Targeting TCTP as a new therapeutic strategy in castration-resistant prostate cancer. Mol Ther 2012; 20: 2244-56.